

# Surface analysis of 4-aminothiophenol adsorption at polycrystalline platinum electrodes

*Belinda I. Rosario-Castro<sup>1</sup>, Estevao R. Fachini<sup>1</sup>, Enid J. Contés<sup>1</sup>, Marla E. Pérez-Davis<sup>2</sup>, and  
Carlos R. Cabrera<sup>1</sup>*

<sup>1</sup>University of Puerto Rico, Río Piedras Campus, Graduate Chemistry Department, PO Box  
23346, San Juan, Puerto Rico 00931-3346

<sup>2</sup>NASA John H. Glenn Research Center, Electrochemistry Branch, 21000 Brookpark Road,  
Cleveland, Ohio 44135

---

<sup>1</sup> Corresponding author e-mail: [marla.e.perez-davis@grc.nasa.gov](mailto:marla.e.perez-davis@grc.nasa.gov)

<sup>2</sup> Corresponding author e-mail: [ccabrera@cnet.upr.edu](mailto:ccabrera@cnet.upr.edu)

Formation of self-assembled monolayer (SAM) of 4-aminothiophenol (4-ATP) on polycrystalline platinum electrodes has been studied by surface analysis and electrochemistry techniques. The 4-ATP monolayer was characterized by cyclic voltammetry (CV), Raman spectroscopy, reflection absorption infrared (RAIR) spectroscopy, and X-ray photoelectron spectroscopy (XPS). Cyclic voltammetry (CV) experiments give an idea about the packing quality of the monolayer. RAIR and Raman spectra for 4-ATP modified platinum electrodes showed the characteristic adsorption bands for neat 4-ATP indicating the adsorption of 4-ATP molecules on platinum surface. The adsorption on platinum was also evidenced by the presence of sulfur and nitrogen peaks by XPS survey spectra of the modified platinum electrodes. High resolution XPS studies and RAIR spectrum for platinum electrodes modified with 4-ATP indicate that molecules are sulfur-bonded to the platinum surface. The formation of S-Pt bond suggests that ATP adsorption gives up an amino terminated SAM. Thickness of the monolayer was evaluated via angle-resolved XPS (AR-XPS) analyses. Derivatization of 4-ATP SAM was performed using 16-Br hexadecanoic acid.

## **1. Introduction**

Self-assembled monolayers (SAMs) are formed through a spontaneous adsorption of molecules onto a substrate surface from a precursor solution. Formation of organic monolayers by self-assembly is directed by a specific interaction between a terminal functional group and the surface. This method has been extensively used for solid surface modification because is a simple, versatile, and convenient way to define the chemical composition and structure of a surface. SAMs have been used for molecular recognition<sup>1</sup>, to alter wetting properties of the surface<sup>2-4</sup>, for electron transfer studies,<sup>5</sup> electrocatalysis,<sup>6</sup> and corrosion protection.<sup>7-9</sup>

Assemblies based on alkanethiols are the most extensively studied self-assembled monolayers. Highly ordered SAMs of alkanethiols have been prepared on a variety of electrode metals, such as silicon<sup>10-11</sup>, silver<sup>12</sup>, copper<sup>8-9</sup>, gold<sup>13-14</sup>, and platinum<sup>15-17</sup>. The strength of the bond formed between the thiol sulfur and the metal<sup>18</sup> allows additional functional groups in the adsorbing molecule with no obstruction of the self-assembly of the molecules through the sulfur. The formation of a densely packed monolayer is also critical to obtain a single functional group exposed on the external surface.<sup>16</sup> An assembly terminated with a desired function provides a supporting structure for further chemical derivatization.<sup>17,19</sup> For the attachment of additional molecules or layers to the modified surfaces, coupling agents, such as acid chlorides, anhydrides and carbodiimides have been used. Researchers have particular interest on amino-terminated monolayers, since they have been used for several applications such as the attachment of carbon nanotubes on metal surfaces<sup>20-21</sup>, and for the binding of biomolecules, like DNA<sup>22-24</sup>. Amino-terminated monolayers have also being used for the development of electrochemical sensors for biomolecules. Raj, et. al., performed the electrochemical transformation of 4-ATP SAM to obtained a confined redox active diimine for electrocatalytic sensing of NADH on gold substrate.<sup>19, 25</sup>

This work discusses results obtained from spectroscopic and electrochemical techniques used to characterize the self-assembly of 4-aminothiophenol (4-ATP) over polycrystalline platinum electrodes. Electrochemical characterization served to study the packing quality of the 4-ATP assembly. Reflection-absorption infrared (RAIR), Raman, and X-ray photoelectron (XPS) spectroscopies results suggest a successful adsorption of 4-ATP as well as the attachment of the molecules through sulfur-platinum bonds. Self- assembled monolayer fabricated based on 4-ATP have significant meaning in terms of the possibility to take advantage of the stability of

the S-metal bonding and the reactivity of the terminal groups for attachment of a new layer via chemical derivatization.

## **2. Experimental Section.**

**2.1. Materials.** 4-aminothiophenol (4-ATP), (Aldrich, 90%), sulfuric acid (Aldrich, 99.999%), potassium ferricyanide ( $K_3Fe(CN)_6$ ) (Aldrich, 99%), potassium chloride (Aldrich, 99.999%), tetrabutylammonium-perchlorate (Fluka, 99%), 16-Br hexadecanoic acid, 4-methylmorpholine (Aldrich, 99%), isobutyl chloroformate (Aldrich, 98%), anhydrous acetonitrile (Aldrich, 99.8%), anhydrous ethanol (Aldrich, 200 proof, 99.5+%). The water used for the experiments was previously distilled and pumped through a nanopure system (Barnstead) to give 18 M $\Omega$  cm nanopure water. Platinum disk electrodes with a diameter of 1.6 mm from Bio-Analytical Systems (BAS) were used for electrochemical measurements and MAXTEK, Inc. platinum electrodes (13 mm of diameter) were used for XPS, and RAIR measurements.

**2.2. Electrochemical cleaning treatment of platinum electrodes and electrochemical characterization of 4-ATP modified platinum (Pt) electrodes.** Electrochemical measurements were performed using a Bipotentiostat AFCBP1 from Pine Instrument Company Grove City. A three electrode cell was employed in all experiments. The reference electrode used was a Ag|AgCl electrode. A platinum mesh electrode was used as the counter electrode. Nanopure water was used to wash the platinum electrodes before and after every electrochemical treatment in sulphuric acid. The working electrode was a platinum disk or a MAXTEK platinum electrode. Cyclic voltammetry (CV) in 0.5 M  $H_2SO_4$ , between -220 mV and 1200 mV vs Ag|AgCl, was performed to verify the cleanliness of both types of electrodes before the modification with 4-ATP SAM. CVs obtained (Figure 2a) are characteristic of clean polycrystalline platinum

surfaces.<sup>26-27</sup> To reuse platinum disk electrodes modified with 4-ATP monolayer, an electrochemical treatment was applied for cleaning. This electrochemical treatment involves repeated cycling in 0.5 M H<sub>2</sub>SO<sub>4</sub> going to very negative potentials (about -800 mV vs. Ag|AgCl). Application of negative potentials helps the desorption of the organic impurities on the electrode surface by hydrogen evolution. Cyclic voltammetry studies for unmodified and 4-ATP modified Pt disk electrodes were performed in 2.5 mM K<sub>3</sub>Fe(CN)<sub>6</sub>/0.1 M KCl electrolyte solutions using a scan rate of 1000 mv/s.

**2.3. Platinum Surface Modification with 4-aminothiophenol (4-ATP): Self-assembled Monolayers (SAMs) Technique.** Self-assembled monolayer was prepared by immersing the Pt electrode in fresh ethanolic solution of 4-aminothiophenol (4-ATP) for a period of 24 hours. Once the deposition is completed, the Pt electrode is removed, rinsed with ethanol, and dried with a slow stream of Ar. Solutions of 4-ATP of 1, 5, and 10 mM concentration were probed.

**2.4. Derivatization of 4-ATP monolayer.** The 16-Br hexadecanoic acid was activated for 1 hour in a solution that contains 80  $\mu$ L of N-methylmorpholine and 100  $\mu$ L of *i*-butyl chlorophormate in DMF. The 4-ATP modified Pt electrode is immersed overnight into the activating solution. The sample is removed and rinse with DMF.

**2.5. X-ray Photoelectron Spectroscopy Analysis.** X-ray photoelectron spectroscopy (XPS) data was obtained using a PHI 5600ci spectrometer with an Al K $\alpha$  X-ray source at 15 kV and 350 W. Spectra were recorded at a take-off angle of 45° and the pass energy of 93.9 eV for the survey analysis and 58.7 eV for high energy resolution studies. Binding energies were corrected to the aliphatic hydrocarbon C1s signal at 285.0 eV. For the determination of the monolayer thickness angle-resolved studies were done at different take-off angles with respect to

the surface plane, specifically 20, 25, 30, 35, 40, 45, 50, and 55°. Software Spartan Version 1.0.1 from Wavefunction, Inc. was used for the 4-ATP molecule length calculation.

**2.6. Infrared Spectroscopy Analysis.** Transmittance spectrum from pure 4-ATP was obtained with a Nicolet Magna IR 750 with a Nic-plan microscope. Specular reflectance for 4-ATP SAMs modified Pt electrode was performed using a Smart SAGA accessory at 80° of incidence in a Nicolet Nexus 870 FT-IR. The spectrum was recorded at 250 scans and 8 cm<sup>-1</sup> of resolution.

**2.7. Raman spectroscopy.** Raman spectra were obtained with a Nicolet Almega Dispersive Raman Spectrometer equipped with a visible raman microscope and a charge couple detector. The excitation wavelength was 785 nm. Recording was carried out at a spectrograph aperture of 25 μm, 5 scans and a 3.8 cm<sup>-1</sup> of resolution.

### **3. Results and Discussion.**

**3.1. Electrochemical measurements.** Cyclic voltammetry (CV) is one of the tools most frequently used to study SAMs on electrodes, because of its high sensitivity attributed to its ability to detect currents from the high rates of mass transfer of redox couples on clean electrodes to small bare sites on a modified electrode.<sup>26</sup> In these experiments, Fe(CN)<sub>6</sub><sup>3-</sup> was used as a redox probe molecule. Figure 1 shows CVs recorded for the redox process of Fe(CN)<sub>6</sub><sup>3-/4-</sup> at clean and modified Pt electrodes using different concentrations of 4-ATP solution to prepare the monolayer. When 1 mM and 5 mM 4-ATP solutions were used for SAM formation, the peak current was reduced but the redox process was still observed. This is evidence of a 4-ATP SAM formed with defects sites, areas of poor packing of the molecules. Mass-transfer of the probe molecule by tunneling through defect sites allow the reduction of Fe(CN)<sub>6</sub><sup>3-</sup> to Fe(CN)<sub>6</sub><sup>4-</sup>. The 4-ATP SAM with a higher packing quality must prevent the probe ions to reach the electrode

surface. As can be seen in Figure 1, SAM prepared using 4-ATP solution with higher concentration (10 mM) presents a substantial decrease in current, demonstrating that a more densely packed monolayer was obtained.

Comparison between the cyclic voltammetry in sulfuric acid of a bare and a 4-ATP modified platinum electrode is also a significant experiment to determine the packing quality. CV in  $\text{H}_2\text{SO}_4$  0.5 M was done for modified electrodes as the same conditions used for uncovered electrodes (Figure 2a). The first and tenth cycle obtained from the same 4-ATP modified electrode (using 10 mM solution) are presented in Figure 2b and 2c, respectively. Notice from the voltammograms that the current at the Pt oxide reduction peak is lower for the modified electrode than the current of the same peak at a clean electrode. Furthermore, the double layer capacitance around 200 mV vs. Ag|AgCl is higher, the peak for Pt oxide formation is shifted to higher potentials, and the hydrogen adsorption/desorption peaks are markedly concealed at the modified electrode voltammogram. These observations are indicative of the 4-ATP molecules adsorption at the surface. Self-assembled 4-ATP monolayer passivates the electrode, substantially inhibiting the electrochemical processes at the platinum surface. In contrast to the first cycle, in the tenth cycle for the modified electrode (Figure 2c) the Pt oxide reduction peak is higher, the double layer capacitance current is diminished, and the hydrogen adsorption/desorption peaks begin to become visible. These observations suggest that the 4-ATP assembly structure is affected under cycling conditions, which possibly promote formation of defect sites by desorption of 4-ATP of molecules. Nevertheless, it is feasible to think that the 4-ATP assembly is stable because there is a shift in hydrogen adsorption/desorption peaks, the peak for Pt oxidation is still shifted to higher potentials, and the Pt oxide reduction peak current is still lower than that for bare Pt electrode.

**3.2. Infrared Spectroscopy Analysis.** Infrared spectroscopy has been widely used to verify the formation of SAMs on metal surfaces. This technique was used to look into the composition and structure of the 4-ATP assembly. Figure 3a and 3b shows IR spectra for neat 4-ATP and a 4-ATP modified platinum electrode, respectively. It is noticeable that the spectrum for 4-ATP modified Pt electrode is qualitatively comparable to the IR spectrum for neat 4-ATP, although there are some differences. One of the differences between these spectra is the absence of the S-H stretch band at  $2550\text{ cm}^{-1}$  in the modified Pt electrode spectrum, suggesting that the sulfur hydrogen bond is substituted by a sulfur-platinum bond. This suggests S-H bonds breakage and the adsorption of 4-ATP molecules to the Pt electrode through the formation of S-Pt bonds. Chemisorption to the surface through the sulfur atoms of the molecules results in the formation of a self-assembly ending with amino groups (which is supported by XPS as will be presented below). The second difference, is that some of the peak positions for 4-ATP adsorb on platinum are shifted to higher energies than those for neat 4-ATP. The peak positions for both the 4-ATP self-assembly on Pt and the pure substance spectra are presented in Table 1. Pure 4-ATP peak position for antisymmetric  $\text{NH}_2$  stretching mode at  $3432\text{ cm}^{-1}$ , CH stretching mode at  $3026\text{ cm}^{-1}$ , and CH bending mode at  $819\text{ cm}^{-1}$  are shifted to  $3450\text{ cm}^{-1}$ ,  $3030\text{ cm}^{-1}$ , and  $826\text{ cm}^{-1}$ , respectively, for 4-ATP assembly. Although the shift in peak positions is not understood at all, this has been attributed to intramolecular lateral interactions within the assembly.<sup>28-29</sup> According to the selection rules for RAIR spectroscopy, only vibration modes with a dipole moment perpendicular to the metallic surface are observed. In our case, all peaks produce by both, vibrations that are parallel and perpendicular to the main molecular axis observed for neat 4-ATP, were also observed for the 4-ATP self-assembled monolayer. Therefore, it is possible that

there is an appropriate angle between molecule axis and metallic surface, which allow the detection of both types of vibration modes.

**3.3. Raman Spectroscopy.** Raman spectroscopy technique is similar to IR spectroscopy, since it also produces a spectral fingerprint unique to a molecule. Figure 4a shows the expected spectrum for a pure sample of 4-ATP with its characteristics bands, which respective values are showed in Table 2. Some of these bands are also present in the spectrum obtained for a 4-ATP modified Pt electrode shown in Figure 4b. These spectra serve as additional evidence of the 4-ATP adsorption on the Pt electrodes surface.

**3.4. X-Ray Photoelectron Spectroscopy (XPS) analysis.** XPS is another technique used to study the composition of SAM modified surfaces. Figures 5a and 5b shows XPS survey spectra for an uncoated and a 4-ATP modified Pt electrode, respectively. Photoemission peaks attributed to nitrogen and sulfur atoms are present in the spectrum of the modified electrode, which are not present in the unmodified Pt electrode spectrum. This is indicative of the adsorption of 4-ATP molecules on the electrode. Figure 6a shows high resolution spectra for the carbon regions of an unmodified and a 4-ATP modified platinum electrode acquired under the same instrumental conditions. The carbon signal for the modified electrode is higher than the same signal for the unmodified electrode. This increase in peak is due to the detection of carbon atoms from the aromatic ring of 4-ATP SAM. Figure 6b shows XPS multiplex spectra for Pt region for unmodified and 4-ATP modified electrode (same instrumental conditions). The Pt signal of the 4-ATP modified electrode is lower than the signal for the unmodified one, because 4-ATP adsorption is preventing the detection of the Pt 4f electron. From the elemental composition analysis (see Table 3) of the 4-ATP assembly, atomic ratios can be calculated. The

experimental atomic ratios C:N = 6.99:1, C:S = 6.89:1, and S:N = 1.01:1 are consistent, within experimental error, with the theoretical values for the 4-ATP molecule.

The curve-fitted high-resolution XPS spectrum at C 1s region (Figure 7a) obtained for 4-ATP modified Pt electrode, presents two major peaks. The peaks at 284.5 eV, and 285.5 eV are attributable to the aromatic C—C, (and C<sub>arom</sub>—S), and C<sub>arom</sub>—N, respectively. These values are comparable with those found in the literature<sup>30</sup>. The third peak presented at 291.0 eV is the shake-up line due to a shake-up process that involves the energy of the  $\pi \rightarrow \pi^*$  transition.

Although it is well-known that thiol compounds forms self-assemblies through S-metal bonding, it is possible that in the 4-ATP assembly some molecules are adsorbed through an interaction between N atoms and the Pt surface. The curve fitting for N 1s and S 2p high-resolution spectra should reveal the chemical nature of the 4-ATP adsorption on platinum electrodes. For the N 1s high-resolution spectrum curve fitting (Figure 7b), only one peak was observed at 399.3 eV, which is characteristic of a neutral amino group<sup>30</sup>. Also, only one sulfur species was observed for the curve fitting of the high-resolution spectrum of S2p region shown in Figure 7c. The doublet at 163.4 eV can be assigned to a thiolate formation on the surface of the platinum surface<sup>31</sup>. These results support IR results, indicating that the adsorption of 4-ATP molecules to the surface occurs through sulfur bonding upon cleavage of the S-H bond. The formation of a 4-ATP assembly composed of just a monolayer is possible, since no more than a single species was found for N and S atoms. There is no evidence of bilayer formation through bonding between two molecules. XPS data evidence the formation of a 4-ATP monolayer on platinum, which contains amino terminal groups.

Angle-resolved XPS measurements have been used to define 4-ATP monolayer thickness and molecular orientation. The monolayer thickness,  $d$ , could be calculated from a plot of  $\ln$

$[I_{ks}(\theta) / I_{0s}(\theta)]$  versus  $1/\cos \theta$ , where  $(-d/\lambda)$  equals the slope of the linear regression. The slope of this attenuation curve of a 4-ATP modified Pt electrode (shown in Figure 8) is  $-1.8732$ , resulting a thickness of  $8.05 \text{ \AA}$ , which is reasonable since the calculated length of 4-ATP molecule is  $6.959 \text{ \AA}$ .

**3.5. Derivatization of 4-ATP monolayer.** To corroborate the reactivity of the amino terminal group of the 4-ATP SAM, 4-ATP modified Pt surfaces were further derivatized with the compound 16-Br hexadecanoic acid. Characteristic peaks that suggest amide bonding are listed in Table 5. The infrared spectrum for this derivatization is shown in Figure 9. A strong band that appears at  $3326 \text{ cm}^{-1}$  could be attributed to the  $\nu\text{NH}$  vibration.<sup>32</sup> The most important band to support the formation of amide bonds is the  $\nu \text{C=O}$  band, also called Amide I band, appears at  $1680 \text{ cm}^{-1}$ .<sup>32</sup> The  $\delta\text{NH}$  and  $\nu\text{C-N}$  frequencies fall close together and therefore interact. That interaction results in the CNH vibrations called amide II and amide III. For the SWNTs modified Pt surface the amide II and amide III bands appear at  $1551$  and  $1306 \text{ cm}^{-1}$ , respectively.<sup>32</sup> These results suggest that a new layer was attached to the existing monolayer via chemical derivatization, opening the possibility to use 4-ATP/Pt system for the attachment of a variety of biomolecules or even carbon nanotubes.

#### 4. Conclusions

The surface analysis of the 4-ATP modified Pt surface, presents evidence of adsorption. RAIR studies indicate that the 4-ATP is absorbed to the platinum surface through the sulfur, forming a S-Pt bond and giving up an amino terminated self-assembled monolayer. On the other hand, from XPS spectra studies is possible to corroborate the S-Pt bonding results obtained from RAIR. The appearance of all RAIR peaks produced by both, parallel and perpendicular

vibrations to the main molecular axis at the 4-ATP self-assembled monolayer spectra, suggest that the molecules are absorbed with a specific angle respect to the metallic surface, which allow the detection of both types of vibration modes. Formation of a densely packed monolayer from the 4-ATP 10 mM solution is supported by ferrocyanide CVs studies, which indicates that 4-ATP/Pt system is free of mass transfer effects. The binding of single-wall carbon nanotubes on Pt surfaces through the free-amino groups of 4-ATP SAM is currently under investigation in our laboratories.

**Acknowledgment.** We are grateful to the Materials Characterization Center of the University of Puerto Rico for the IR and XPS analyses, to Eunice Wong for her assistance on the Raman analysis at NASA Glenn Research Center, to Dr. José A. Prieto for his help in the calculation of 4-ATP molecule length. BIRC would like to acknowledge the financial support from NASA Graduate Student Researcher Program fellowship (NGT3-52381).

**Table 1. Peak Position of IR Spectra of neat 4-ATP and Self-Assembled 4-ATP Monolayer**

<i>mode assignment</i>	<i>pure substance (transmission IR) / cm<sup>-1</sup></i>	<i>self assembled monolayer (RAIR) / cm<sup>-1</sup></i>
$\nu_a\text{NH}_2$	3432	3450
$\nu_s\text{NH}_2$	3358	3352
$\nu\text{NH}_2$	3213	3201
$\nu\text{CH}_{\text{arom}}$	3026	3030
$\nu\text{SH}$	2554	-
$\nu\text{CH}_{\text{overtone}}$	1888	1884
$\nu\text{CC}$	1620	1620
$\nu\text{CC}$	1595	1593
$\nu\text{CC}$	1496	1494
$\nu\text{CC}$	1447	1423
$\nu\text{CN}$	1284	1292
$\nu\text{CS}_{\text{arom}}$	1090	1089
$\delta\text{CH}_{\text{arom}}$	820	826

**Table 2. Peak Position of Raman Spectra for neat 4-ATP and for Self-Assembled 4-ATP Monolayer**

<i>mode assignment</i>	<i>pure substance (transmission IR) / cm<sup>-1</sup></i>	<i>self assembled monolayer (RAIR) / cm<sup>-1</sup></i>
$\nu\text{CH}_{\text{arom}}$	3048	3048
$\nu\text{SH}$	2544	-
$\nu\text{CC}$	1593	1590
$\nu\text{CS}_{\text{arom}}$	1087	1085
$\delta\text{CH}_{\text{arom}}$	818	820

**Table 3. XPS Atomic Concentrations for 4-ATP Modified Platinum Surface**

<b>Species</b>	<i>C1s</i>	<i>N1s</i>	<i>O1s</i>	<i>S2p</i>
<b>Concentration (%)</b>	74.82	10.71	2.28	10.86

**Table 4. Peak Position of RAIR Spectrum for 4-ATP modified Pt surface derivatized with 16-Br hexadecanoic acid.**

<i>mode assignment</i>	<i>16-HA/4-ATP (RAIR) / cm<sup>-1</sup></i>
$\nu\text{NH}$	3326
$\nu\text{CH}$	2927
$\nu\text{CH}$	2855
$\nu\text{CO}$ (Amide I)	1680
$\nu\text{CN} + \delta\text{NH}$ (Amide II)	1551
$\nu\text{CNH}$ (Amide III)	1306

## References

- (1) Chailapakul, O.; Crooks, R. M. *Langmuir* **1985**, *11*, 1329.
- (2) Laibinis, P. E.; Whitesides, G. M. *J. Am. Chem. Soc.* **1992**, *113*, 1990.
- (3) Laibinies, P. E.; Nuzzo, R. G.; Whitesides, G. M. *J. Phys. Chem.* **1992**, *96*, 5097.
- (4) Fukishima, F.; Seki, S.; Nishikawa, T.; Takiguchi, H.; Tamada, K.; Abe, K.; Colorado, R.; Graupe, M.; Shmakova, O. E.; Lee, T. R. *J. Phys. Chem. B* **2000**, *104*, 7417.
- (5) Dong, X. D.; Lu, J.; Cha, C. *J. Electroanal. Chem.* **1995**, *388*, 195.
- (6) Cheng, L.; Pacey, G. E.; Cox, J. A. *Electrochimica Acta* **2001**, *46*, 4223.
- (7) Meage, I.; Jaehne, E.; Henke, A.; Adler, H-J. P.; Bram, C.; Jung, C.; Stratmann, M. *Progress in Org. Coatings* **1997**, *34*, 1.
- (8) Tremont, R.; De Jesus-Cardona, H.; Garcia-Orozco, J.; Castro, R. J.; Cabrera, C. R. *J. Appl. Electrochem.* **2000**, *30*, 737.
- (9) Tremont, R.; Cabrera, C. R. *J. Appl. Electrochem.* **2002**, *32*, 783.
- (10) Brandow, S. L.; Chen, M. S.; Aggarwal, R.; Dulcey, C. S.; Calvert, J. M.; Dressick, W. J. *Langmuir* **1999**, *15*, 5429.
- (11) Wei, Z. Q.; Wang, C. F.; Zhu, C. F.; Zhou, C. Q.; Xu, B.; Bai, C. L. *Surface Science* **2000**, *459*, 401.
- (12) Sang Woo Han, Seung Joon Lee, Kwan Kim. *Langmuir* **2001**, *17*, 6981.
- (13) Xiao, X.; Wang, B.; Zhang, C.; Yang, Z.; Loy, M. M. T. *Surface Science* **2001**, *472*, 41.
- (14) Azzaroni, O.; Vela, M. E.; Martin, H.; Hernandez Creus, A.; Andreasen, G.; Salvarezza, R. C. *Langmuir* **2001**, *17*, 6647.
- (15) Clavilier, J.; Svetličić, V.; Zutić, V. *J. Electroanal. Chem.* **1996**, *402*, 129.
- (16) Brito, R.; Rodriguez, V. A.; Figueroa, J.; Cabrera, C. R. *J. Electroanal. Chem.* **2002**, *520*, 47.
- (17) Brito, R.; Tremont, R.; Feliciano, O.; Cabrera, C.R. *J. Electroanal. Chem.* **2003**, *540*, 53.
- (18) Bard, A. J. In *Integrated Chemical System*; John Wiley & Sons: New York, 1994.
- (19) Raj, C. R.; Kitamura, F.; Ohsaka, T. *Langmuir* **2001**, *17*, 7378.
- (20) Liu, Z.; Sehn, Z.; Zhu, T.; Hou, S.; and Ying, L.; Shi, Z.; Gu, Z. *Langmuir* **2000**, *16*, 3569.
- (21) Nan, X.; Gu, Z.; Liu, Z. *J. Colloid and Interface Sci.* **2002**, *245*, 311.
- (22) Brockman, J. M.; Frutos, A. G.; Corn, R. M. *J. Am. Chem. Soc.* **1999**, *121*, 8044.
- (23) Frutos, A. G.; Brockman, J. M.; Corn, R. M. *Langmuir* **2000**, *16*, 2192.
- (24) Smith, E. A.; Wanat, M. J.; Cheng, Y.; Barreira, S. V. P.; Frutos, A. G.; Corn, R. M. *Langmuir* **2001**, *17*, 2502.
- (25) Raj, C. R.; Ohsaka, T. *Langmuir* **2001**, *3*, 633.
- (26) Finklea, H. O. In *Encyclopedia of Analytical Chemistry*; Robert A. Meyers, R. A., Ed.; John Wiley & Sons Ltd: Chichester, 2000.
- (27) Allara, D. L.; Unzo, R.G. *Langmuir* **1985**, *1*, 45.
- (28) Bradshaw, A. M.; Schweizer, E. In *Advances in Spectroscopy. Spectroscopy of Surfaces*; Hester, R. E., Clark, R. J. H., Eds.; Wiley: New York, 1988; Vol. 16, pp 413-488.
- (29) Willis, R. F.; Lucas, A. A.; Mahan, G. D. *The Chemical Physics of Solid Surfaces and Heterogeneous Catalysis*; King, d. A., Woodruff, D. P., Eds.; Elsevier: Amsterdam, 1981; Vol. 2, pp 67-100.
- (30) Lukkari, J.; Kleemola, K.; Meretoja, M.; Ollonqvist, T.; Kankare, J. *Langmuir* **1998**, *14*, 1705.

---

(31) Bandyopadhyay, K.; Vijayamohanan, K.; Venkataramanan, M.; Pradeep, T. *Langmuir* **1999**, *15*, 5314.

(32) Colthup, N. B.; Daly, L. H.; and Wiberley, S. E. In *Introduction to Infrared and Raman Spectroscopy*, 3<sup>rd</sup> Ed.; Academic Press: Boston, 1990.

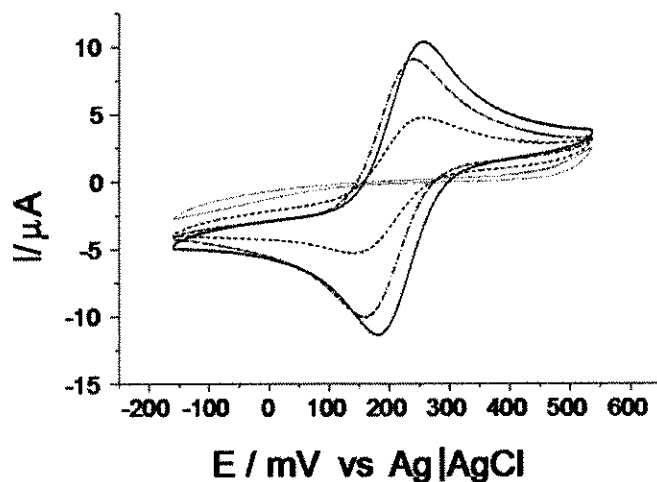


**Figure 1.** CVs in a solution of 2.5 mM  $\text{K}_3\text{Fe}(\text{CN})_6$  at a scan rate of 1000 mV/s for (a —) an unmodified Pt electrode, and 4-ATP modified Pt electrodes prepared by immersing in (b ---) 1 mM, (c ----) 5 mM, and (d ·····) 10 mM 4-ATP solutions

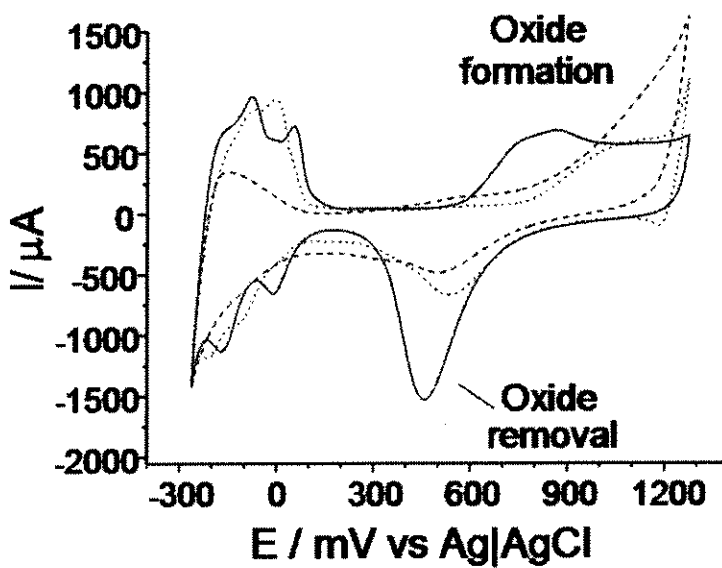


**Figure 2.** Cyclic voltammograms of Pt MAXTEK electrodes in 0.5 M  $\text{H}_2\text{SO}_4$  solution. (a —) Voltammogram for clean Pt MAXTEK electrode. Scan rate  $100 \text{ mV s}^{-1}$ . (b ---) First and (c ·····) tenth cycle of a 4-ATP modified Pt electrode.

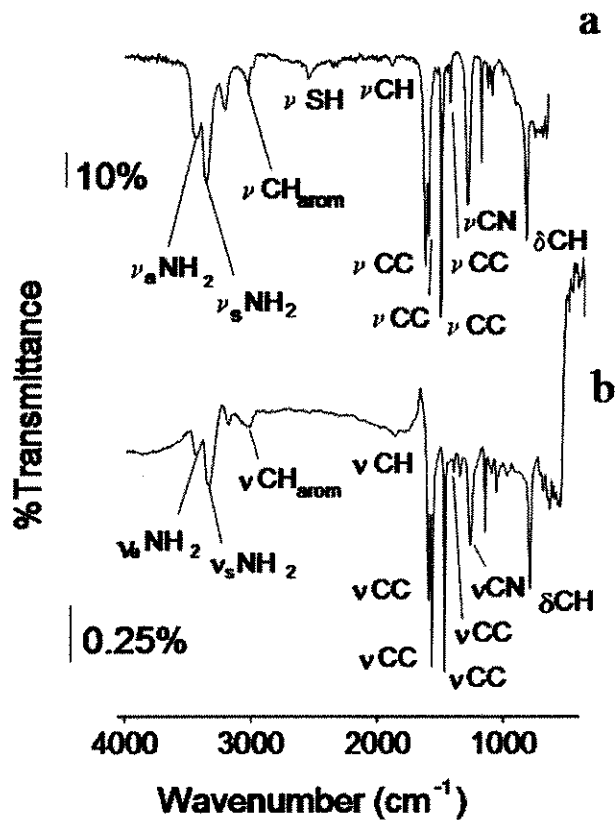


**Figure 3.** Fourier-transforms / infrared spectroscopy (FTIR): (a) Transmittance spectrum for pure 4-ATP sample, and (b) reflection-absorption spectrum for a 4-ATP modified Pt electrode.

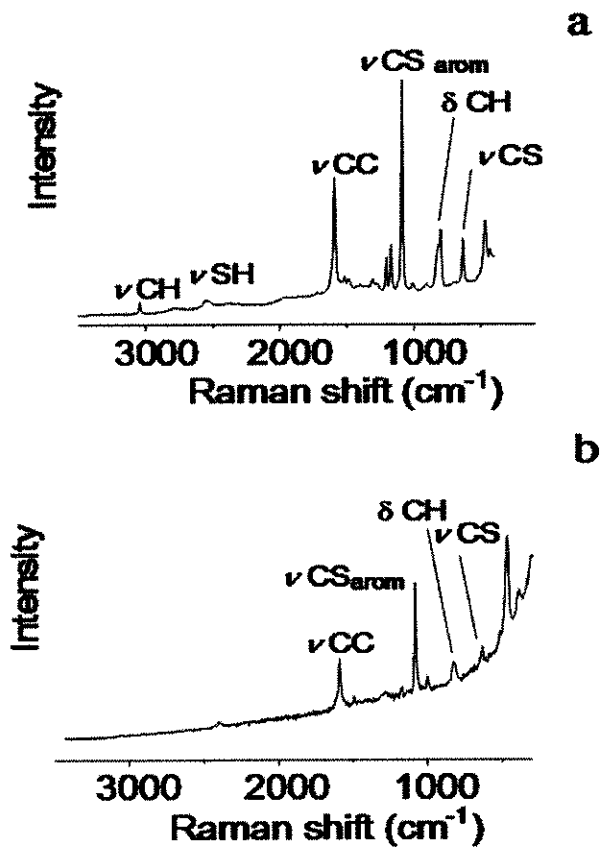


**Figure 4.** Raman spectra for (a) a pure 4-ATP sample, (b) 4-ATP modified Pt electrode.

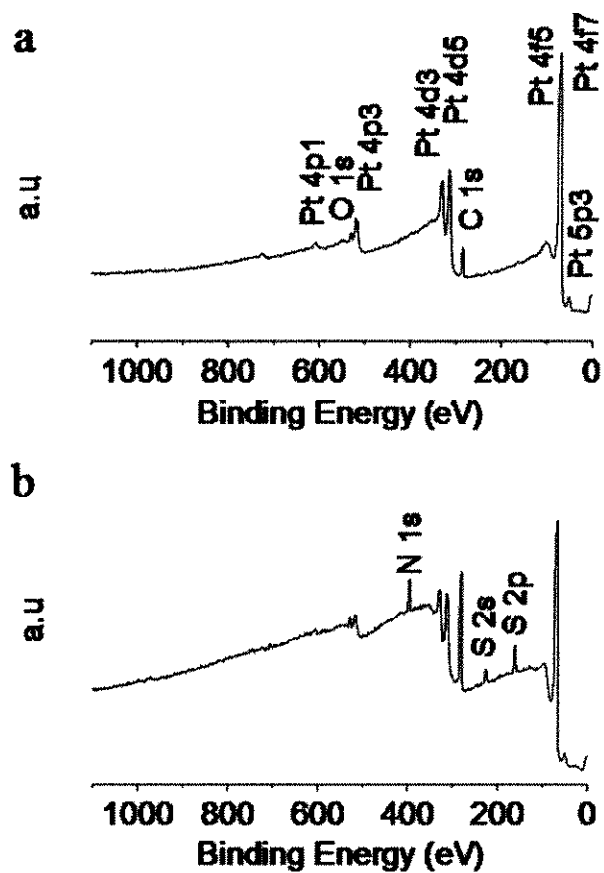


**Figure 5.** XPS spectra for (a) unmodified Pt electrode immersed in anhydrous ethanol for 24 hours, and (b) 4-ATP modified Pt electrode.

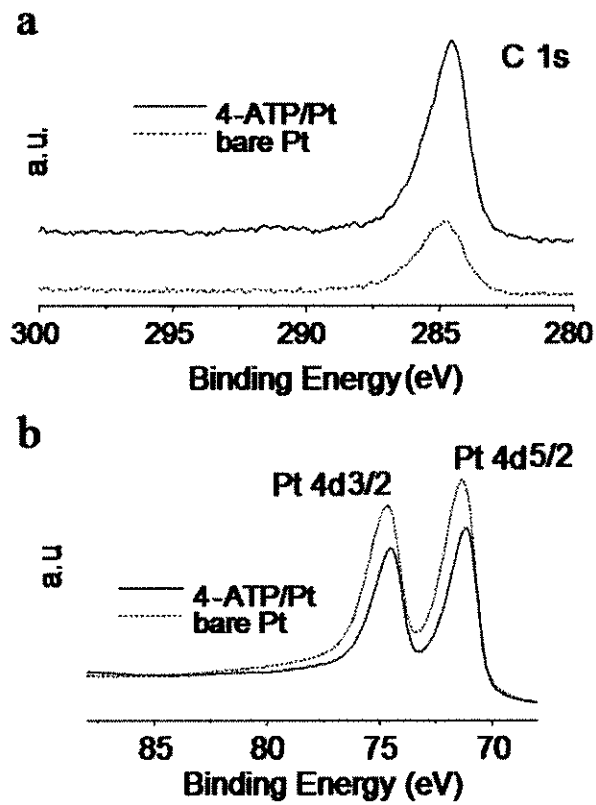


**Figure 6.** High resolution XPS spectra for unmodified and 4-ATP modified electrodes at (a) carbon region and (b) platinum region. The same XPS experimental conditions were used.

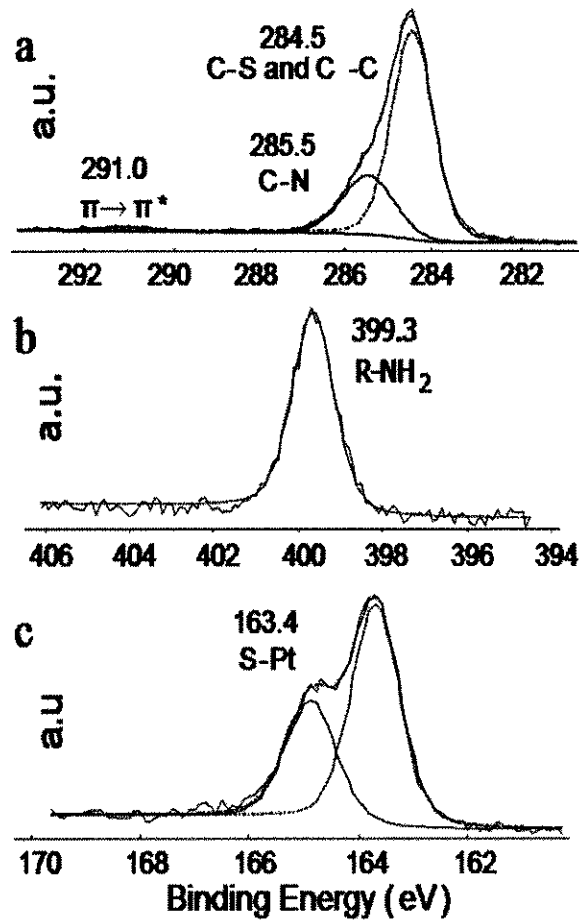


**Figure 7.** Curve-fitted high-resolution XPS spectra for the (a) C1s, (b) N1s, and (c) S2p regions for a 4-ATP modified platinum electrode. The same XPS instrumental conditions were used.

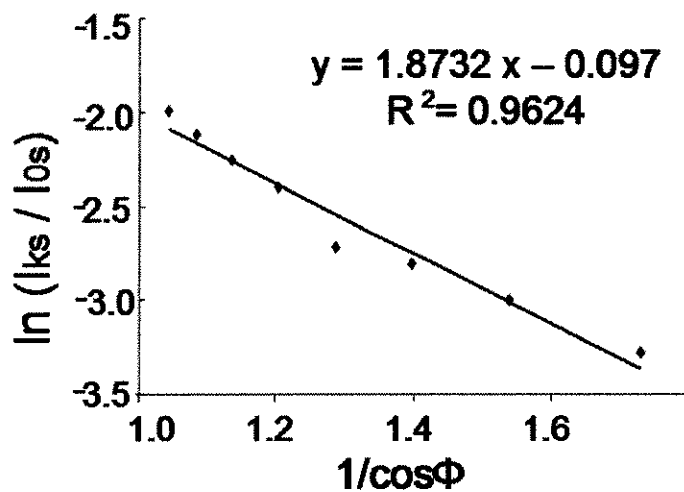


**Figure 8.** Depth Profile of 4-aminothiophenol SAM on Pt surface.

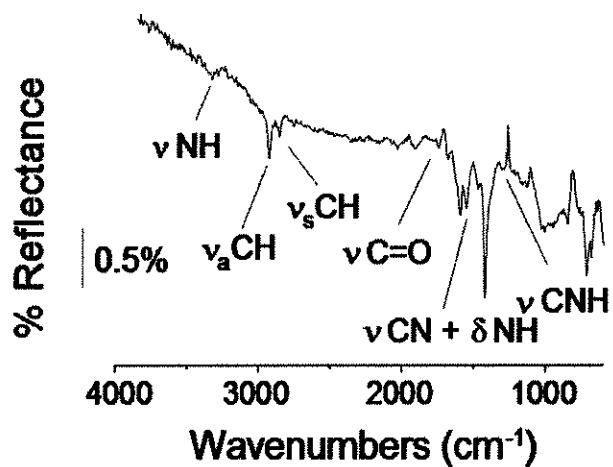


**Figure 9.** Reflection-absorption infrared spectrum for a 4-ATP modified Pt electrode derivatized with 16-Br hexadecanoic acid.